

1 **Lung-to-ear sound transmission does not improve**
2 **directional hearing in green treefrogs (*Hyla cinerea*)**

3
4 **Jakob Christensen-Dalsgaard¹, Norman Lee², Mark A. Bee^{3,4,‡}**

5
6 ¹Department of Biology, University of Southern Denmark, 5230 Odense M, Denmark

7
8 ²Department of Biology, St. Olaf College, Northfield, MN 55057

9
10 ³Department of Ecology, Evolution, and Behavior, University of Minnesota - Twin Cities, St.
11 Paul, MN 55126

12
13 ³Graduate Program in Neuroscience, University of Minnesota - Twin Cities, Minneapolis, MN
14 55455

15
16
17 ‡ Author for correspondence (mbee@umn.edu)

18
19
20 Running title: Directional hearing in green treefrogs

21
22 Keywords: Acoustic communication, Directional hearing, Internally-coupled ears, Mate choice,
23 Sound localization, Spatial hearing

24
25 **SUMMARY STATEMENT**

26 Contrary to prevailing views on the mechanisms of hearing in frogs, the lung-to-ear pathway for
27 sound transmission does not improve directional hearing in these vociferous vertebrates.

28 **ABSTRACT**

29 Amphibians are unique among extant vertebrates in having middle ear cavities that are
30 internally coupled to each other and to the lungs. In frogs, the lung-to-ear sound transmission
31 pathway can influence the tympanum's inherent directionality, but what role such effects might
32 play in directional hearing remain unclear. In this study of the American green treefrog (*Hyla*
33 *cinerea*), we tested the hypothesis that the lung-to-ear sound transmission pathway functions to
34 improve directional hearing, particularly in the context of interspecific sexual communication.
35 Using laser vibrometry, we measured the tympanum's vibration amplitude in females in
36 response to a frequency modulated sweep presented from 12 sound incidence angles in
37 azimuth. Tympanum directionality was determined across three states of lung inflation (inflated,
38 deflated, reinflated) both for a single tympanum in the form of the vibration amplitude difference
39 (VAD) and for binaural comparisons in the form of the interaural vibration amplitude difference
40 (IVAD). The state of lung inflation had negligible effects (typically less than 0.5 dB) on both
41 VADs and IVADs at frequencies emphasized in the advertisement calls produced by conspecific
42 males (834 Hz and 2730 Hz). Directionality at the peak resonance frequency of the lungs (1558
43 Hz) was improved by $\cong 3$ dB for a single tympanum when the lungs were inflated versus
44 deflated, but IVADs were not impacted by the state of lung inflation. Based on these results, we
45 reject the hypothesis that the lung-to-ear sound transmission pathway functions to improve
46 directional hearing in frogs.

47 INTRODUCTION

48 Vocal communication is of prime importance for successful reproduction in most frogs (Gerhardt
49 and Huber, 2002; Narins et al., 2007; Ryan, 2001). In many species, stationary male signalers
50 produce loud advertisement calls to attract females to their calling site or territory (Schwartz and
51 Bee, 2013; Wells and Schwartz, 2007). As an intended receiver, a gravid female must perform
52 two critical perceptual tasks in order to reproduce (Gerhardt and Bee, 2007). First, she must
53 recognize that a male's call belongs to the set of calls of her species based on analyzing its
54 spectral and temporal properties. Second, she must localize and approach the source of the
55 calls using phonotaxis (approach toward sound), often while navigating a spatially complex
56 microhabitat under low light levels, such as a vegetated wetland at night. Both perceptual tasks
57 – sound pattern recognition and sound source localization – commonly take place in noisy
58 breeding choruses that create unfavorable signal-to-noise ratios for communication (Bee, 2012,
59 2015; Bee and Christensen-Dalsgaard, 2016; Vélez et al., 2013).

60 Previous studies have shown that frogs exhibit highly directional phonotaxis toward
61 conspecific calls, with jumps and head orientations often directed to within a few degrees of the
62 sound source (Feng et al., 1976; Gerhardt and Rheinlaender, 1982; Jørgensen and Gerhardt,
63 1991; Rheinlaender et al., 1979; Shen et al., 2008; Ursprung et al., 2009). In addition, frogs
64 have good source localization acuity and angle discrimination for sounds originating within the
65 frontal field (e.g., $\pm 45^\circ$ from the midline)(Caldwell and Bee, 2014; Klump and Gerhardt, 1989).
66 Although directional phonotaxis is a critically important component of frog reproductive behavior,
67 we still lack a complete understanding of the mechanisms underlying directional hearing and
68 sound source localization in these animals (Bee and Christensen-Dalsgaard, 2016; Eggermont,
69 1988; Klump, 1995; Rheinlaender and Klump, 1988).

70 Two anatomical features of the frog's auditory system are currently believed to play key
71 functional roles in directional hearing: their internally coupled ears and their lungs (Bee and
72 Christensen-Dalsgaard, 2016). The free-field directionality of the frog's tympanum has been
73 investigated in a few species, in all cases showing a directional response at frequencies where
74 diffraction of sound around the head is unimportant (Caldwell et al., 2014; Jørgensen, 1991;
75 Jørgensen and Gerhardt, 1991; Jørgensen et al., 1991; Vlaming et al., 1984). Most likely, a part
76 of the increased directionality is produced by acoustical interaction of the two tympana, because
77 the air-filled middle ears of most frogs are internally coupled through the mouth cavity via wide
78 and permanently open Eustachian tubes (Christensen-Dalsgaard, 2005, 2011; van Hemmen et
79 al., 2016; but see Gridi-Papp et al., 2008). With this physical arrangement, each tympanum
80 functions as a pressure-difference receiver with an inherently directional vibration response to

81 sound originating from different positions in azimuth, although sound input to both ears is still
82 required for accurate sound localization (Feng et al., 1976). Frogs also possess an accessory
83 pathway for sound transmission between the body wall overlying the lungs and the internally-
84 coupled middle ears (Ehret et al., 1990, 1994; Narins et al., 1988). The lungs can influence the
85 magnitude of the tympanum's directionality, with these effects being more pronounced at
86 frequencies near the resonance frequency of the lungs (Jørgensen, 1991; Jørgensen et al.,
87 1991; see also reviews in Christensen-Dalsgaard, 2005, 2011). While internally coupled ears
88 also play functional roles in directional hearing in some other vertebrates, such as lizards and
89 crocodylians (Bierman et al., 2014; Carr and Christensen-Dalsgaard, 2016; Christensen-
90 Dalsgaard and Manley, 2008; Christensen-Dalsgaard et al., 2011), and in some invertebrates,
91 such as crickets and katydids (Römer, 2015; Römer and Schmidt, 2016), the frog's lung-to-ear
92 sound transmission pathway appears to be unique among vertebrates, and its precise
93 contribution to directional hearing remains uncertain (Bee and Christensen-Dalsgaard, 2016). At
94 present, each tympanum's directional response is thought to result from the interaction of sound
95 impinging directly on its external surface and sound that indirectly reaches its internal surface
96 from the other tympanum via the internal coupling and from the lungs via the glottis. Although
97 there is strong empirical and theoretical support for the role of internal coupling in determining
98 the tympanum's directionality, and there is clear evidence that the lungs contribute to the
99 tympanum's response to sound, how these multiple inputs – direct from the free field, indirect
100 via the opposite tympanum, and indirect via the lungs – act together to influence directional
101 hearing in frogs is not well understood

102 In this study of the American green treefrog, *Hyla cinerea* (Schneider, 1799), we tested
103 the hypothesis that the lung-to-ear sound transmission pathway functions to improve directional
104 hearing, particularly in the context of interspecific sexual communication. The auditory and vocal
105 communication systems of green treefrogs have been well studied in terms of basic auditory
106 perception and physiology (Buerkle et al., 2014; Ehret and Capranica, 1980; Ehret and
107 Gerhardt, 1980; Ehret et al., 1983; Gerhardt and Höbel, 2005; Klump et al., 2004; Megela-
108 Simmons et al., 1985; Moss and Simmons, 1986; Penna et al., 1992); sound pattern
109 recognition, species recognition, and mate choice (Allan and Simmons, 1994; Gerhardt, 1974,
110 1978a, b, 1981, 1987, 1991; Gerhardt et al., 1987; Höbel and Gerhardt, 2003; Lee et al., 2017;
111 Simmons, 1988; Simmons et al., 1993); and sound source localization (Feng et al., 1976; Klump
112 et al., 2004; Rheinlaender et al., 1979). In contrast to the extensive data on neurophysiology
113 and behavior, only two studies have investigated the biophysics, and in particular the
114 directionality, of the tympanum in green treefrogs (Michelsen et al., 1986; Rheinlaender et al.,

115 1981). However, neither study investigated the role of the lung-to-ear sound transmission
116 pathway in determining the directionality of the tympanum.

117 We used laser vibrometry to quantify the contribution of the lung-to-ear pathway in
118 shaping the inherent directionality of the tympanum's vibration amplitude response. To this end,
119 we investigated how both the *vibration amplitude difference* (VAD) for a single tympanum and
120 the *interaural vibration amplitude difference* (IVAD) varied as functions of lung inflation in
121 response to free-field stimulation. The VAD refers to the difference between vibration
122 amplitudes of the measured tympanum across different angles of sound incidence at a
123 particular frequency. Thus, as a measure of directionality, the VAD represents the physical
124 change in how a single tympanum responds to sounds presented from different angles in
125 azimuth. As a complement to the VAD, the IVAD is a computed measure of binaural disparity
126 that is more relevant to questions of directional hearing because it quantifies the difference
127 between the vibration amplitudes of the left and right tympana when sound of a particular
128 frequency originates from a particular sound incidence angle (Jørgensen et al., 1991). Hence,
129 the IVAD estimates the difference in input through the auditory periphery on the left and right
130 sides of the animal and, therefore, more closely approximates the information available to the
131 auditory nervous system for computing the azimuthal direction of a sound source (Bee and
132 Christensen-Dalsgaard, 2016).

133

134 **MATERIALS AND METHODS**

135 **Animals**

136 All animal procedures were approved by the Institutional Animal Care and Use Committee of the
137 University of Minnesota (#1401-31258A) and complied with the NIH *Guide for the Care and Use*
138 *of Laboratory Animals* (8th Edition). Subjects were 25 adult female green treefrogs of unknown
139 age (mean \pm SD snout-to-vent length = 53.61 \pm 3.50 mm, range = 47.7 to 59.2 mm; mean \pm SD
140 mass = 12.71 \pm 2.92 g, range = 8.3 to 17.6 g; mean \pm SD interaural distance = 14.08 \pm 1.00
141 mm, range = 11.9 to 15.7 mm). They were collected in amplexus in July 2015 from ponds
142 located at the East Texas Conservation Center in Jasper County, Texas, U.S.A. (30°56'46.15"N,
143 94°7'51.46"W). Animals were returned within 48 hours of collection to the laboratory at the
144 University of Minnesota, where they were housed on a 12-hour light:dark cycle, provided with
145 access to perches and refugia, fed a diet of vitamin-dusted crickets, and given ad libitum access
146 to fresh water.

147 All laser measurements of an individual subject were made during a single recording
148 session of less than two hours during which they were immobilized with an intramuscular

149 injection of succinylcholine chloride (5 µg/g) into the thigh. We allowed subjects to regulate their
150 own lung volume undisturbed over the 5-10 minutes during which the immobilizing agent took
151 effect. After full immobilization was achieved, the state of lung inflation resembled that observed
152 in unmanipulated frogs sitting in a natural posture based on visual inspection of lateral body wall
153 extensions (see Caldwell et al., 2014). Hereafter, we refer to this state of lung inflation as the
154 “inflated” condition. We also took laser measurements in two additional states of lung inflation.
155 To create the “deflated” condition, we expressed the air from the animal’s lungs by gently
156 depressing the lateral body wall while using the narrow end of a small, plastic pipette tip to hold
157 the glottis open. For the “reinflated” condition, we attempted to return the lungs to their natural
158 level of inflation observed prior to manual deflation by gently blowing air by mouth through a
159 pipette with its tip located just above the closed glottis; the movement of air was sufficient to
160 open the glottis and inflate the lungs. We have previously shown these procedures to be
161 effective at deflating and reinflating the lungs (Caldwell et al., 2014; Lee et al., 2020). By
162 necessity, measurements were always made first in the inflated condition followed by the
163 deflated condition and then the reinflated condition. We facilitated cutaneous respiration while
164 subjects were immobilized by periodically applying water to the dorsum to keep the skin moist.
165 Animals that resumed buccal pumping during a recording session received a second, half dose
166 of succinylcholine chloride. In the analyses reported below, four of 25 subjects were excluded
167 (final $N = 21$) because we could not confidently confirm differences in their state of lung inflation
168 across treatments based on visual inspection of lateral body wall extensions.

169

170 **Apparatus**

171 Laser measurements were made inside a custom-built, semi-anechoic sound chamber (inside
172 dimensions: 2.9 m [L] × 2.7 m [W] × 1.9 m [H], Industrial Acoustics Company, North Aurora, IL).
173 The inside walls and ceiling of the chamber were lined with Sonex acoustic foam panels (Model
174 VLW-60; Pinta Acoustic, Inc. Minneapolis, MN) to reduce reverberations. The chamber’s floor
175 was covered in low-pile carpet. During recordings, subjects sat in a typical posture in the
176 horizontal plane atop an acoustically transparent, cylindrical pedestal (30-cm tall, 7-cm
177 diameter) made from wire mesh (0.9-mm diameter wire, 10.0-mm grid spacing). A raised arch of
178 thin wire was used to support the tip of the subject’s mandible, such that its jaw was parallel to
179 the ground. We mounted the base of the pedestal to a horizontal, 70-cm long piece of Unistrut®
180 (Unistrut, Harvey, IL) that extended to the center of the sound chamber from a mount on a
181 vibration isolation table (Technical Manufacturing Corporation, Peabody, MA) positioned against
182 an inside wall of the sound chamber. We covered the Unistrut and vibration isolation table with

183 the same acoustic foam that lined the walls and ceiling of the chamber. In this configuration, the
184 top of the pedestal was 120 cm above the floor of the sound chamber at its center. The laser
185 vibrometer used for measurements (PDV-100, Polytech, Irvine, CA) was mounted at the same
186 height on the vibration isolation table from which the subject pedestal was mounted and was
187 positioned 70° to the animal's right relative to the position of its snout (0°).

188

189 **Acoustic stimulation and laser measurements**

190 We presented subjects with a frequency-modulated (FM) sweep (44.1 kHz, 16-bit) broadcast at
191 a sound pressure level (SPL re 20 µPa, fast, C-weighted) of 85 dB from each of 12 sound
192 incidence angles (0° to 330° in 30° steps) in azimuth. The direction in which the animal's snout
193 pointed was taken to be 0°. Thus, an angle of +90 corresponds to the animal's right side, which
194 was ipsilateral to the laser, and an angle of 270° (equivalent to -90°) corresponds to the
195 animal's left side, which was contralateral to the laser. The stimulus had a total duration of 195
196 ms, with linear onset and offset ramps of 10 ms. Over the 175-ms steady-state portion of its
197 amplitude envelope, the stimulus increased linearly in frequency from 0.2 to 7.5 kHz. We
198 amplified the stimulus (Crown XLS1000, Elkhart, IN) and broadcast it through a single speaker
199 (Mod1, Orb Audio, New York, NY) that was positioned 50 cm away from the approximate center
200 of a subject's head (measured from the intersection of the midline and the interaural axis) as it
201 sat on the pedestal. The speaker was suspended from the ceiling of the sound chamber by a
202 rotating arm fashioned from steel pipe and covered in acoustic foam that allowed us to put the
203 speaker at any azimuthal position relative to the subject. The speaker was at the same height
204 above the chamber floor as the subject. We used a G.R.A.S. 40SC probe microphone (G.R.A.S.
205 Sound & Vibration A/S, Holte, Denmark) to record stimuli at the position of the tympanum. The
206 tip of a flexible probe tube was positioned approximately 2 mm from the edge of the subject's
207 right tympanum during recordings. We amplified the output of the probe microphone using an
208 MP-1 microphone pre-amplifier (Sound Devices, Reedsburg, WI) and recorded its output using
209 an external digital and analog data acquisition (DAQ) device (NI USB 6259, National
210 Instruments, Austin, TX).

211 Just prior to making recordings, we calibrated the stimulus separately for each speaker
212 position using a Brüel & Kjær Type 2250 sound level meter (Brüel & Kjær Sound & Vibration
213 Measurement A/S, Nærum, Denmark) and a Brüel & Kjær Type 4189 ½-inch condenser
214 microphone. Signal levels for calibration and playback were controlled using a programmable
215 attenuator (PA5, Tucker-Davis Technologies, Alachua, FL). For calibration measurements, the
216 microphone of the sound level meter was suspended from the ceiling of the sound chamber by

217 an extension cable (AO-0414-D-100) so that the tip of the microphone was located at the
218 position occupied by a subject's head during recordings.

219 For each subject, the vibration amplitude of the right tympanum was first recorded in the
220 inflated condition, beginning at a randomly determined location around the subject. Responses
221 at each successive angle were recorded after repositioning the speaker in a counterclockwise
222 direction. At each speaker location, we recorded the tympanum's response to 20 repetitions of
223 the stimulus (1.5-s stimulus period). After recording responses from the 12th and final speaker
224 location in the inflated condition, we repeated the above procedure to measure the tympanum in
225 the deflated condition beginning at the same randomly determined starting location used in the
226 naturally inflated condition. Following all measurements in the deflated condition, this procedure
227 was then repeated a third and final time in the reinflated condition.

228 We measured the vibration amplitude of the animal's right tympanum by focusing the
229 laser on a small (45- μ m to 63- μ m diameter), retroreflective glass bead (P-RETRO-500,
230 Polytech, Irvine, CA) placed at the center of the right tympanum. We digitized (44.1 kHz, 16 bit)
231 the analog output of the laser using the NIDAQ device, which we controlled using MATLAB[®]
232 (v.2014a, MathWorks, Natick, MA) running on an OptiPlex 745 PC (Dell, Round Rock, TX).
233 Tympanum vibration spectra were calculated from the acquired laser signals in MATLAB using
234 the pwelch function (window size = 256, overlap = 50%). Vibration spectra were corrected for
235 small directional variation in the sound spectrum by calculating transfer functions between
236 tympanum vibrations and sound at the tympanum's external surface. This was done by dividing
237 the tympanum vibration spectrum by the sound spectrum recorded by the probe microphone
238 (i.e., by subtraction of dB values).

239

240 **Data analysis**

241 We computed the VAD at a particular frequency as the maximum difference in the vibration
242 amplitudes (in dB) of the measured tympanum that occurred across different angles of sound
243 incidence. Computed this way, the VAD is a measure of the directional response of a single
244 tympanum. In contrast, the IVAD, which is a measure of binaural disparity, was computed for a
245 particular frequency from measurements of a single ear by assuming bilateral symmetry and
246 computing the difference based on the correct corresponding angles. For example, the IVAD for
247 30° was computed as the difference between the vibration amplitudes measured at 30° and
248 330° (i.e., -30°) relative to the midline at 0°. VADs and IVADs were computed based on laser
249 measurements made while the animals' lungs were inflated and again after both deflating and
250 reinflating the lungs. We restricted analyses of VADs and IVADs to those measured across a 4-

251 octave range between 300 Hz and 4800 Hz to avoid artificially large values that were
252 sometimes observed to occur well outside the range of typical tympanum sensitivity when the
253 laser signal was near its internal noise floor. We used linear interpolation to determine the
254 values of VADs and IVADs occurring between fixed angles of stimulation.

255 We focused our statistical analyses of VADs and IVADs on three frequencies of
256 biological relevance: two spectral peaks emphasized in the advertisement calls produced by
257 conspecific males and the peak resonance frequency of the lungs of females. Similar to related
258 species in the genus *Hyla* (Gerhardt, 2001, 2005; Gerhardt et al., 2007), male green treefrogs
259 produce an advertisement call with a frequency spectrum consisting of two prominent spectral
260 peaks that are analogous to the formant frequencies present in human vowel sounds (Lee et al.,
261 2017; Oldham and Gerhardt, 1975). The lower spectral peak is important for long-distance
262 communication and source localization (Gerhardt, 1976; Klump et al., 2004; Rheinlaender et al.,
263 1979), whereas the higher spectral peak may be more important in sexual selection via female
264 mate choice (Gerhardt, 1976, 1981). Females have robust preferences for calls containing both
265 spectral peaks (Lee et al., 2017). Based on analyses of a sample of 457 advertisement calls (\cong
266 20 calls from each of 23 males), Lee et al. (2020) reported the mean (\pm SD) frequencies of the
267 lower and higher spectral peaks to be 834 ± 14 Hz and 2730 ± 34 kHz, respectively. The mean
268 frequency of the “valley” between these two spectral peaks was 1653 ± 39 Hz. Using laser
269 vibrometry, Lee et al. (2020) determined the mean peak frequency of the lung resonance in a
270 sample of 10 females to be 1558 Hz (range: 1400 Hz to 1850 Hz).

271 A two-way repeated-measures analysis of variance (rmANOVA) was used to assess
272 differences in the magnitude of the VAD as a function of lung inflation (inflated, deflated, and
273 reinflated) at three fixed frequencies (834 Hz, 1558 Hz, and 2730 Hz). We used a three-way
274 rmANOVA to assess differences in the magnitude of the IVAD as a function of lung inflation
275 (inflated, deflated, and reinflated) at the same three fixed frequencies (834 Hz, 1558 Hz, and
276 2730 Hz) and at five fixed sound incidence angles (30° to 150° in 30° steps). We additionally
277 report the results from quadratic contrasts for all main effects of lung inflation given the general
278 expectation based on previous studies that the directionality observed with the lungs inflated
279 should decrease in the deflated condition and be restored in the reinflated condition. For all
280 rmANOVAs, we report F values (and their unadjusted degrees of freedom) based on the
281 Greenhouse and Geiser (1959) correction for possible violations of sphericity and partial η^2
282 values as measures of effect size. We used $\alpha = 0.05$ to determine statistical significance. All
283 statistical analyses were conducted using SPSS v21.

284

285 **RESULTS**

286 In all three lung inflation conditions, the tympanum had a bandpass frequency response and
287 was most sensitive to frequencies between about 1000 Hz and 5000 Hz across most angles of
288 sound incidence (Fig. 1). In both the inflated (Fig. 1A) and reinflated (Fig. 1C) conditions, there
289 was also a prominent “dip” in the vibration amplitude spectrum between approximately 1400 Hz
290 and 2200 Hz. This dip corresponded closely with the peak resonance frequency of the lungs
291 (1558 Hz) and was largely absent in the deflated condition (Fig. 1B). Across frequencies,
292 vibration amplitudes were greatest at ipsilateral angles of +60° to +120° (on the animal’s right
293 side) compared with the corresponding contralateral angles of -60° to -120° (on the animal’s left
294 side). The tympanum’s greatest directionality, as indicated by the differences in vibration
295 amplitude between ipsilateral and contralateral angles, occurred in the frequency region of the
296 dip (Fig. 1). These general trends are evident both in the tympanum’s vibration amplitude
297 response for two representative frogs and in the mean vibration amplitude of the right
298 tympanum averaged across all individuals (Fig. 1). Reinflation of the deflated lungs was more
299 successful in some animals than in others at restoring the dip in the vibration amplitude
300 spectrum (cf. Frog 1 and Frog 2 in Fig. 1C). Consequently, the directionality associated with the
301 dip was, on average, slightly less pronounced in the reinflated condition compared with the
302 inflated condition. We cannot rule out the possibility that changes in the volume of air in the
303 mouth cavity resulting from manipulations of lung inflation also contribute to differences between
304 the inflated and reinflated states.

305

306 **Vibration amplitude differences (VADs)**

307 With inflated lungs, the tympanum’s maximum directionality – as measured by the maximum
308 VAD at any frequency across any two sound incidence angles – was 15.5 dB and occurred at a
309 frequency of 1486 Hz and between angles of +99° (ipsilateral) and -49° (contralateral) (Table 1).
310 The maximum VAD decreased by 4 dB when the lungs were deflated and was largely restored
311 (within 1 dB) when the lungs were reinflated (Table 1). Differences in the mean frequency and
312 mean sound incidence angles at which the maximum VAD occurred were generally small (e.g.,
313 < 240 Hz and < 40°) across the three states of lung inflation (Table 1).

314 We assessed the impacts of lung inflation on VADs using a 3 lung inflation (inflated,
315 deflated, reinflated) × 3 frequency (834 Hz, 1558 Hz, 2730 Hz) rmANOVA. Recall that the
316 lowest (834 Hz) and highest (2730 Hz) frequencies correspond to the two prominent spectral
317 peaks in conspecific advertisement calls, and the intermediate frequency (1558 Hz)
318 corresponds to the peak resonance frequency of the inflated lungs. This analysis revealed

319 significant main effects of both lung inflation ($F_{2,40} = 6.18$, $P = 0.006$, partial $\eta^2 = 0.24$) and
320 frequency ($F_{2,40} = 52.98$, $P < 0.001$, partial $\eta^2 = 0.73$), and their two-way interaction was also
321 significant ($F_{4,80} = 5.55$, $P = 0.002$, partial $\eta^2 = 0.22$). The quadratic contrast for the main effect
322 of lung inflation was also significant ($F_{1,20} = 14.94$, $P = 0.001$, partial $\eta^2 = 0.43$). Averaged
323 across all three frequencies, the mean ($\pm 95\%$ CI) VADs were lowest in the deflated condition
324 (8.5 ± 0.7 dB) and higher and more similar in the inflated (9.8 ± 0.7 dB) and reinflated ($10.1 \pm$
325 1.1 dB) conditions. Averaged across all three states of lung inflation, mean ($\pm 95\%$ CI) VADs
326 were largest at a frequency of 1558 Hz (11.6 ± 1.1 dB), smallest at 2730 Hz (6.8 ± 0.4 dB), and
327 intermediate at 834 Hz (10.1 ± 0.9 dB). The two-way interaction between lung inflation and
328 frequency resulted because the impacts of lung inflation were more pronounced at the
329 intermediate frequency of 1558 Hz compared with call frequencies of 834 Hz and 2730 Hz (Fig.
330 2). At 1558 Hz, the mean VAD was 3.4 dB and 2.6 dB lower in the deflated condition compared
331 with the inflated and reinflated conditions, respectively (Fig. 2). In contrast, the differences in
332 mean VADs across the three states of lung inflation were less than 1.8 dB, and most were less
333 than 0.4 dB, at frequencies of 834 Hz and 2730 Hz (Fig. 2).

334

335 **Interaural vibration amplitude differences (IVADs)**

336 The left-right asymmetries present in measures of vibration amplitude (Fig. 1) are also reflected
337 in the magnitudes of the IVADs plotted as heatmaps in Figure 3. IVADs in all states of lung
338 inflation were generally greatest between about 1000 Hz and 3000 kHz and between $+45^\circ$ and
339 $+135^\circ$, with the largest IVADs occurring near 1600 Hz at 90° (Figure 3). Figure 4 depicts IVADs
340 as functions of lung inflation at the two call frequencies and the lung resonance frequency, and
341 Figure 5 illustrates how these IVADs varied as a function of sound incidence angle. We
342 evaluated how IVADs varied as a function of lung inflation at fixed combinations of sound
343 incidence angle and frequency using a 3 lung inflation (inflated, deflated, reinflated) \times 5 angle
344 (30° , 60° , 90° , 120° , 150°) \times 3 frequency (834 Hz, 1558 Hz, 2730 Hz) rmANOVA. There were
345 large and significant main effects of angle ($F_{4,80} = 113.2$, $P < 0.001$, partial $\eta^2 = 0.87$) and
346 frequency ($F_{2,40} = 41.5$, $P < 0.001$, partial $\eta^2 = 0.68$), and there was a significant two-way
347 interaction between angle and frequency ($F_{8,160} = 26.8$, $P < 0.001$, partial $\eta^2 = 0.57$). As
348 illustrated in the polar plots in Figure 5, IVADs tended to be highest near sound incidence
349 angles close to 90° and to decrease to 0 dB as the sound source was positioned closer to the
350 axis of the midline (0° and 180°). Mean ($\pm 95\%$ CI) IVADs, averaged across sound incidence
351 angles and states of lung inflation, were higher at the peak resonance frequency of the lungs
352 (1558 Hz: 6.6 ± 1.6 dB) and lower at the two frequencies emphasized in conspecific mating calls

353 (834 Hz: 5.2 ± 1.2 dB; 2730 Hz: 3.5 ± 0.7) (Figs. 4 & 5). The largest IVAD occurred at 90° and
354 1558 Hz, and the smallest IVAD occurred at 30° and 2730 Hz (Fig. 5).

355 In contrast to the effects of sound incidence angle and frequency, the state of lung
356 inflation had no significant effects on IVADs (Fig. 4): both the main effect of lung inflation ($F_{2,40} =$
357 0.37 , $P = 0.680$, partial $\eta^2 = 0.02$) and the quadratic contrast for the main effect of lung
358 inflation ($F_{1,20} = 0.48$, $P = 0.495$, partial $\eta^2 = 0.02$) were small and nonsignificant, as were the
359 two-way interactions between lung inflation and both angle ($F_{8,160} = 1.40$, $P = 0.245$, partial $\eta^2 =$
360 0.07) and frequency ($F_{4,80} = 0.45$, $P = 0.710$, partial $\eta^2 = 0.02$), as well as the three-way
361 interaction between these variables ($F_{16,320} = 0.96$, $P = 0.53$, partial $\eta^2 = 0.05$). The overall
362 mean ($\pm 95\%$ CIs) IVADs, averaged over angle and frequency, were 5.2 ± 1.1 dB, 5.0 ± 1.2 dB,
363 and 5.1 ± 1.1 dB in the inflated, deflated, and reinflated conditions.

364 The difference in IVADs between the inflated and deflated states of lung inflation were
365 close to 0 dB at all combinations of frequency and sound incidence angle. This outcome is
366 apparent in the heatmap shown in Figure 6A, which illustrates the mean differences in IVADs
367 between the inflated and deflated states across sound incidence angles and frequency in
368 relation to the average spectrum of conspecific calls. The nearly uniform, pale green color of the
369 heatmap corresponds to an IVAD near 0 dB and indicates that the state of lung inflation had a
370 negligible impact on IVAD magnitude. At the two spectral peaks emphasized in conspecific
371 calls, and at the peak resonance frequency of the lungs, the mean ($\pm 95\%$ CIs) IVAD
372 differences between the inflated and deflated conditions included 0 dB at nearly all angles of
373 sound incidence (Fig. 6B).

374 Table 2 summarizes the magnitudes of the maximum IVAD in each lung inflation
375 condition along with the frequencies and sound incidence angles at which they occurred. On
376 average, the magnitude of the maximum IVAD was similar in the inflated (12.4 dB; Table 2) and
377 reinflated (12.5 dB; Table 2) conditions, and it was approximately 1 dB less in the deflated
378 condition (11.2 dB; Table 2). Across the three lung inflation conditions, the mean frequencies at
379 which the maximum IVAD was observed varied over a narrow range between 1579 Hz and
380 1690 Hz (Table 2), which is close to the mean peak resonance frequency of the lungs (1558
381 Hz). The mean angles at which the maximum IVAD was observed varied between 82.9° in the
382 inflated condition and 100.0° in the deflated condition, and the median angle for all three states
383 of lung inflation was 90° (Table 2).

384
385

386 **DISCUSSION**

387 The goal of this study was to test the hypothesis that the lung-to-ear sound transmission
388 pathway functions to improve directional hearing. We found little evidence to support this
389 hypothesis, and no evidence that sound input through the lungs might function to improve the
390 localization of conspecific advertisement calls. Both the directionality of a single tympanum, as
391 measured by the VAD, and the impacts of lung inflation on this measure of directionality were
392 greater at frequencies near the peak resonance frequency of the lungs than at frequencies
393 emphasized in conspecific calls. When measured as binaural disparities in the form of IVADs,
394 directionality was again highest at frequencies near the peak resonance frequency of the lungs,
395 but the state of lung inflation had little impact on directionality at these frequencies. Most
396 importantly, the state of lung inflation had a negligible impact on directionality, measured either
397 for a single ear (VADs) or as binaural disparities (IVADs), at the frequencies emphasized in
398 conspecific calls. Based on these measurements, we conclude that the lung-to-ear sound
399 transmission pathway probably plays no significant role in directional hearing in the context of
400 localizing conspecific advertisement calls in green treefrogs.

401 Before discussing the role of the frog's lungs in directional hearing in more detail, it is
402 first worth considering how our findings on tympanum directionality relate to previous work in
403 green treefrogs and other frog species. In their study of green treefrogs, Feng et al. (1976) were
404 the first to demonstrate that female frogs rely on binaural cues to localize calling males. Sound
405 localization was completely disrupted when one tympanum was covered with a thin layer of
406 silicone grease, with frogs repeatedly turning in the direction of their unaltered ear (see also
407 Rheinlaender et al., 1979). Based on measures of jump angles during phonotaxis in closed-loop
408 tests, Rheinlaender et al. (1979; see also Klump et al., 2004) showed that sound localization in
409 green treefrogs was highly accurate in azimuth, with a mean jump angle (i.e., the angle between
410 the direction of the speaker and the direction of a jump) of 16.1° and a modal jump angle falling
411 between 3° to 7° . Angles of head orientation (i.e., the angle between the direction of the
412 speaker and the direction in which the frog's snout pointed) were even smaller (mean = 8.4° ;
413 mode = 0° to 3°), indicating even better directional resolution than that based on jumps. Lateral
414 head scanning prior to jumps improved jump accuracy in azimuth (mean jump angle = 11.8° ;
415 Rheinlaender et al., 1979), and scanning with the head raised above the horizontal plane was
416 crucial for localizing elevated sources (Gerhardt and Rheinlaender, 1982). Klump and Gerhardt
417 (1989) showed in open loop tests that the closely related barking treefrog (*Hyla gratiosa*) was
418 capable of true angle discrimination, not just lateralization, and could discriminate angles
419 differing by as little as 15° in azimuth within the frontal sound field ($\pm 45^\circ$), a result later

420 corroborated by Caldwell and Bee (2014) for Cope's gray treefrog (*Hyla chrysoscelis*).
421 Rheinlaender et al. (1981) reported a directional sensitivity at 90° of about 4 dB in green
422 treefrogs based on midbrain neural responses to a 1000 Hz tone. Using laser vibrometry to
423 measure the tympanum's response directly, Michelsen et al. (1986) later reported an mean
424 IVAD at 90° closer to 9 dB in response to tones between 1000 Hz and 3000 Hz. These values
425 generally accord well with the IVADs reported in the present study: at the call frequencies of 834
426 Hz and 2730 Hz, the mean (\pm 95% CI) IVADs at 90° were 4.4 ± 0.6 dB and 4.4 ± 0.7 dB,
427 respectively, while that at the lung resonance of 1558 Hz was 8.9 ± 1.0 dB (Fig. 5). By
428 comparison, sound pressure levels measured at the external surfaces of the tympana were
429 typically ± 1 dB in the range of 1000 Hz to 3000 Hz (Michelsen et al., 1986). Because we found
430 the state of lung inflation had no impact on the magnitudes of IVADs, the larger binaural
431 disparities in the tympanum's response most likely arise from interaural coupling of the middle
432 ears. In an electrophysiological study of sound localization in green treefrogs, Feng and
433 Capranica (1978) reported that about 42% of cells in the superior olivary nucleus and 88% of
434 cells in the inferior colliculus (torus semicircularis) were sensitive to binaural input, with the vast
435 majority of binaural cells exhibiting EI responses in which the cells were excited by contralateral
436 stimulation and inhibited by ipsilateral stimulation. Some EI neurons in the inferior colliculus
437 were sensitive to small binaural disparities of just 1 dB to 2 dB, suggesting that IVADs on the
438 order of 4 dB to 8 dB would be more than sufficient to drive directional neural responses
439 subserving sound localization behavior in this species. Interaural time differences of up to 1.3
440 ms in auditory nerve responses to the amplitude modulation in natural calls may produce
441 additional cues for sound localization (Klump et al., 2004).

442 As illustrated in Table 3, the present study also corroborates four broad patterns
443 reported in previous biophysical studies of tympanum directionality in both closely related
444 congeneric species as well as more distantly related species. First, the frog tympanum exhibits
445 a bandpass frequency response with a characteristic "dip" in vibration amplitude at intermediate
446 frequencies (Caldwell et al., 2014; Chung et al., 1981; Ho and Narins, 2006; Jørgensen, 1991;
447 Jørgensen and Gerhardt, 1991; Jørgensen et al., 1991; Pinder and Palmer, 1983; Wilczynski et
448 al., 1987). Second, the dip in tympanum sensitivity occurs at frequencies that are not
449 emphasized in the spectra of conspecific advertisement calls (Caldwell et al., 2014; Jørgensen,
450 1991; Jørgensen and Gerhardt, 1991; Jørgensen et al., 1991). Third, the dip typically coincides
451 with the frequencies of maximum tympanum directionality (Jørgensen, 1991; Jørgensen and
452 Gerhardt, 1991; Jørgensen et al., 1991). And finally, the frequency range of the dip corresponds
453 closely to the peak resonance frequency of the lungs (Caldwell et al., 2014; Jørgensen, 1991;

454 Jørgensen et al., 1991). Green treefrogs exemplify all four patterns. The tympanum was most
455 responsive in the frequency range of about 1000 Hz to 5000 Hz, and the tympanum's transfer
456 function had a prominent dip between approximately 1400 Hz and 2200 Hz when the lungs
457 were inflated. The dip frequency range fell between the lower (834 Hz) and upper (2730 Hz)
458 spectral peak of the advertisement call and included the peak resonance frequency of the lungs
459 (1558 Hz; range: 1400 Hz to 1850 Hz; Lee et al., 2020). The maximum VAD was 15.5 dB and
460 occurred at 1486 Hz, which is between the two spectral peaks of the call and within the
461 frequency range of the dip in the tympanum's transfer function. By comparison, VADs were
462 smaller (approximately 5 to 10 dB) at the frequencies emphasized in conspecific advertisement
463 calls. These patterns are similar to those documented in other species studied to date (Table 3),
464 including eastern gray treefrogs (*Hyla versicolor*, Hylidae), Cope's gray treefrogs (*H.*
465 *chrysoscelis*, Hylidae), barking treefrogs (*H. gratiosa*, Hylidae), coqui frogs (*Eleutherodactylus*
466 *coqui*, Eleutherodactylidae), and grass frogs (*Rana temporaria*, Ranidae). The three taxonomic
467 families represented in this pool of species are members of two superfamilies, Hyloidea (Hylidae
468 and Eleutherodactylidae) and Ranoidea (Ranidae), that last shared a common ancestor some
469 155 million years ago (Kumar et al., 2017). Thus, the patterns observed in the frog species
470 studied to date may be both ancient and taxonomically widespread, and perhaps characteristic
471 of the more than 5000 species of frog in the suborder Neobatrachia within the Anura. Species in
472 other suborders have not been investigated.

473 Our findings extend this earlier work by showing that sound transmission through the
474 lungs does not improve directional hearing and thus does not function in localizing conspecific
475 calls. This conclusion is at odds with early suggestions that the lungs might improve localization
476 of conspecific calls (Ehret et al., 1990) and with previous studies suggesting that sound
477 transmission through the lungs improves the tympanum's directionality (Jørgensen, 1991;
478 Jørgensen et al., 1991). Previous studies demonstrating an impact of the lungs on directional
479 hearing have inferred changes in VADs in small numbers of subjects (e.g., $N \leq 6$) after applying
480 thick layers of petroleum jelly to the body wall to dampen sound transmission to inflated lungs
481 (Jørgensen, 1991; Jørgensen et al., 1991) or after directly manipulating the state of lung
482 inflation (Caldwell et al., 2014; Jørgensen, 1991). In their study of the coqui frog, for example,
483 Jørgensen et al. (1991) reported that dampening sound transmission through the body wall with
484 petroleum jelly eliminated the dip in the tympanum's transfer function and decreased the
485 tympanum's vibration amplitude by 10-15 dB at low frequencies typical of the "co" note of the
486 advertisement call. Interestingly, they also report that the maximum directionality (inferred from
487 the VAD) was "only slightly reduced" in treated frogs (p. 228, Jørgensen et al., 1991). In green

488 treefrogs, deflating the lungs decreased the maximum VAD by 4 dB, from 15.5 dB to 11.5 dB
489 (Table 1). Thus, while the lungs influenced the magnitude of the VAD at frequencies near the
490 lung resonance, a large directionality remained in the deflated state, presumably due to the
491 internal coupling of the tympana. These data suggest both a relatively weak influence of lung
492 inflation on interaural transmission gain and that the lungs do not contribute much to interaural
493 coupling and hence to directionality. One important consideration for interpreting these findings
494 based on the VAD is that the VAD measures the directional response of a single tympanum,
495 whereas frogs must use binaural comparisons to localize conspecific calls in azimuth (Feng et
496 al., 1976; Rheinlaender et al., 1979). Hence, IVADs are the more relevant measure of
497 directional hearing because they characterize the binaural disparities in tympanum vibrations
498 that are ultimately used by the nervous system to localize sound sources (Jørgensen et al.,
499 1991). The IVAD can even be seen as a simplified model of interaural comparison in the CNS,
500 assuming that the periphery is symmetrical across the midline (Christensen-Dalsgaard and
501 Manley, 2005). The magnitude of IVADs reported here (e.g., 4 dB to 10 dB) are in line with
502 those reported in earlier studies of coqui frogs (8 dB; Jørgensen et al., 1991), eastern gray
503 treefrogs (e.g., 3 dB to 7 dB; Jørgensen and Gerhardt, 1991), and Cope's gray treefrogs (e.g., 2
504 dB to 5 dB; Caldwell et al., 2014). Like VADs, IVADs tend to be larger at frequencies near the
505 lung resonance and the dip in the tympanum's transfer function and smaller at frequencies
506 emphasized in advertisement calls (Bee and Christensen-Dalsgaard, 2016). However, despite
507 larger IVADs at frequencies intermediate between call frequencies, sound localization
508 performance is actually degraded when signals are modified to emphasize the frequencies of
509 greatest directionality (Jørgensen and Gerhardt, 1991). No previous study has investigated the
510 potential effects the lungs may have on the magnitude of the IVAD. Our data indicate
511 unequivocally that the state of lung inflation has negligible impact on IVADs: differences in
512 IVADs between the inflated and deflated conditions were close to 0 dB across frequency and
513 azimuth. Because IVADs are likely the most important cue for sound localization in frogs, these
514 findings suggest the auditory nervous system receives consistent directional information from
515 the periphery, probably based on the interaural coupling of the tympana, irrespective of the state
516 of lung inflation.

517 To date, no study has investigated the influence of the lungs on phase-related cues for
518 sound localization, such as the magnitude of interaural phase differences (i.e., interaural
519 vibration phase difference, or IVPD) and the corresponding interaural time differences (i.e.,
520 interaural vibration time difference, or IVTD), which might provide cues for call localization in
521 some species, particularly for low-frequency spectral components (Ho and Narins, 2006) or

522 amplitude-modulated signals (Klump et al., 2004). It seems unlikely that phase differences in the
523 spectral components of calls would be useful for call localization in green treefrogs. In their
524 study of the congeneric Cope's gray treefrog (*H. chrysoscelis*), Caldwell et al. (2014) reported
525 that IVPDs were generally similar to or smaller than phase differences at the external surfaces
526 of the two tympana. In that study, IVTDs in frogs with inflated lungs never exceeded 120 μ s and
527 most were less than 60 μ s, even for frequencies as low as 600 Hz. Moreover, as previously
528 noted by Klump et al. (2004), phase locking in the frog auditory nerve is weak at frequencies
529 near the low-frequency component of green treefrogs calls and does not occur at frequencies
530 near the high-frequency component of their calls (Feng et al., 1991; Narins and Hillery, 1938;
531 Narins and Wagner, 1989; Ronken, 1990; Rose and Capranica, 1985). Thus, any influence the
532 lungs may have on the magnitude of IVPDs would likely be inconsequential for directional
533 hearing based on the use of interaural phase cues.

534 The mismatch between the frequencies of maximal tympanum directionality and the
535 frequencies emphasized in conspecific calls has remained paradoxical: why is the tympanum
536 most directional at frequencies not used for communication given the importance of sound
537 localization in frog sexual and social behavior? Several hypotheses have been proposed to
538 explain this apparent paradox. Jørgensen et al. (1991) hypothesized that in coqui frogs (*E.*
539 *coqui*) individuals might be able to tune the maximal directionality of the tympana to the
540 frequency of the "co" note of the advertisement call by adjusting the volume, and hence
541 resonance frequency, of their lungs. While the frequency of maximal directionality can be
542 altered by changing the lung's volume (Jørgensen, 1991), current evidence suggests changes
543 in lung inflation produce relatively small changes. For example, reducing the lung volume from
544 100% to 30% of maximal inflation only changed the lung resonance frequency by 150 Hz in
545 barking treefrogs (*H. gratirosa*) (Jørgensen, 1991). In the present study, deflating the lungs
546 shifted the frequency of the maximum VAD downward by only 231 Hz (from 1486 Hz to 1255
547 Hz; Table 1) and the frequency of the maximum IVAD downward by 300 Hz (from 1550 Hz to
548 1250 Hz; Table 2). Both shifts were insufficient to reach the lower spectral peak of the
549 advertisement call at 834 Hz. These findings suggest the scope for tuning the tympanum's
550 directionality by manipulating lung resonance via volume changes is rather limited. Additional
551 hypotheses for the documented mismatch are that it reflects either an evolutionary adaptation to
552 avoid overlap between call frequencies and the frequencies affected by the lung input because
553 of variability of the lung-induced directionality during the respiratory cycle or a physical
554 constraint between lung resonance frequency and call frequencies (Jørgensen, 1991). Both
555 hypotheses are unsatisfactory. As already noted, even large changes in lung inflation produce

556 only small changes in the frequency of maximal directionality. Moreover, the frog's lungs remain
557 continuously pressurized above atmospheric pressure during the respiratory cycle (De Jongh
558 and Gans, 1969), and they remain inflated for relatively long periods punctuated by brief
559 episodes of ventilation when pulmonary air is expelled and then refilled using an active pump
560 mechanism driven by buccal musculature (Jørgensen et al., 1991). Thus, the acoustical
561 properties of the lung input probably change very little over the respiratory cycle, and frogs
562 probably do not contend with large variability in directionality due to pulmonary respiration.
563 There is also no clear co-dependence between call frequencies and lung resonance frequency,
564 since call frequencies depend on the size and structure of vocal cords and cricoid cartilages,
565 and the lung resonance frequency, measured in the inflated, static situation, is not really
566 relevant in call production, during which the lungs deflate.

567 More recently, Lee et al. (2020) proposed a resolution to the paradoxical mismatch
568 between call frequencies and lung-mediated effects on the frequencies of maximal directionality.
569 They provided evidence from green treefrogs suggesting it is actually the lung-mediated
570 reduction in sensitivity associated with the dip in the tympanum's transfer function, and not
571 enhanced directionality, that is adaptive in the context of communication and environmental
572 noise control. By comparing transfer functions with the lungs inflated versus deflated, they found
573 that the lung resonance creates a directionally tuned notch filter that attenuates the tympanum's
574 vibration amplitude in the frequency range of 1400 Hz to 2200 Hz and predominantly within the
575 contralateral portion of the frontal hemifield. A physiological model of peripheral frequency
576 tuning indicated that these lung-mediated reductions in tympanum sensitivity are restricted to a
577 frequency range where the tuning of the frog's two inner ear organs for transducing airborne
578 sound frequencies, the amphibian and basilar papillae, overlaps at the high sound levels used
579 for communication. Based on these findings, Lee et al. (2020) suggested the lung-to-ear sound
580 transmission pathway functions to sharpen peripheral frequency tuning. They argued that
581 inflated lungs create a mechanism for real-time spectral contrast enhancement (SCE) similar to
582 that implemented in signal processing algorithms in hearing aids and cochlear implants that can
583 improve speech recognition in noise by humans with impaired hearing (Baer et al., 1993;
584 Nogueira et al., 2016; Simpson et al., 1990). For frogs, the end result of spectral contrast
585 enhancement would be a lung-mediated improvement in peripheral matched filtering in the
586 spectral domain, which is believed to play important roles in call recognition as a mechanism to
587 reduce interference from heterospecific signals or environmental noise (Simmons, 2013). To
588 evaluate this possibility, Lee et al. (2020) integrated social network analyses of content-scale
589 citizen science data on frog calling activity with bioacoustic analyses of calls to show that some

590 of the most common species encountered in mixed-species choruses across the green
591 treefrog's geographic range produce calls with prominent spectral peaks in the range of 1400
592 Hz to 2200 Hz. Hence, the lung-to-ear sound transmission pathway may serve an important
593 noise control function in frogs that communicate in mixed species choruses. By showing that the
594 lungs do not improve directional hearing in the context of localizing conspecific calls, the current
595 study suggests alternative adaptive functions of the lung-to-ear sound transmission pathway,
596 such as spectral contrast enhancement (Lee et al., 2020) or hearing protection during calling
597 (Narins, 2016), deserve additional consideration.

598

599 **Acknowledgements**

600 We thank Chris Maldonado of the Texas Parks and Wildlife Division and Gary Calkins of the
601 East Texas Conservation Center for permission to collect frogs under Scientific Permit Number
602 SPR-0410-054; J. Tanner and M. Elson for help collecting frogs; and S. Gupta for assistance
603 with animal husbandry.

604

605 **Competing interests**

606 The authors declare no competing or financial interests.

607

608 **Author contributions**

609 J.C.D., N.L., and M.A.B. designed the experiments, collected and analyzed the data, and co-
610 wrote the manuscript.

611

612 **Funding**

613 This research was supported by a grant from the National Science Foundation (IOS-1452831)
614 to M.A.B.

615

616 **References**

617 **Allan, S. E. and Simmons, A. M.** (1994). Temporal features mediating call recognition
618 in the green treefrog, *Hyla cinerea*: Amplitude modulation. *Animal Behaviour* **47**, 1073-1086.

619 **Baer, T., Moore, B. C. and Gatehouse, S.** (1993). Spectral contrast enhancement of
620 speech in noise for listeners with sensorineural hearing impairment: Effects on intelligibility,
621 quality, and response times. *Journal of Rehabilitation Research and Development* **30**, 49-72.

622 **Bee, M. A.** (2012). Sound source perception in anuran amphibians. *Current Opinion in*
623 *Neurobiology* **22**, 301-310.

- 624 **Bee, M. A.** (2015). Treefrogs as animal models for research on auditory scene analysis
625 and the cocktail party problem. *International Journal of Psychophysiology* **95**, 216-237.
- 626 **Bee, M. A. and Christensen-Dalsgaard, J.** (2016). Sound source localization and
627 segregation with internally coupled ears: The treefrog model. *Biological Cybernetics* **110**, 271-
628 290.
- 629 **Bierman, H. S., Thornton, J. L., Jones, H. G., Koka, K., Young, B. A., Brandt, C.,
630 Christensen-Dalsgaard, J., Carr, C. E. and Tollin, D. J.** (2014). Biophysics of directional
631 hearing in the American alligator (*Alligator mississippiensis*). *The Journal of Experimental
632 Biology* **217**, 1094-1107.
- 633 **Brzoska, J., Walkowiak, W. and Schneider, H.** (1977). Acoustic communication in the
634 grass frog (*Rana t. temporaria* L.): Calls, auditory thresholds and behavioral responses. *Journal
635 of Comparative Physiology A* **118**, 173-186.
- 636 **Buerkle, N. P., Schrode, K. M. and Bee, M. A.** (2014). Assessing stimulus and subject
637 influences on auditory evoked potentials and their relation to peripheral physiology in green
638 treefrogs (*Hyla cinerea*). *Comparative Biochemistry and Physiology A* **178**, 68-81.
- 639 **Caldwell, M. S. and Bee, M. A.** (2014). Spatial hearing in Cope's gray treefrog: I. Open
640 and closed loop experiments on sound localization in the presence and absence of noise.
641 *Journal of Comparative Physiology A* **200**, 265-284.
- 642 **Caldwell, M. S., Lee, N., Schrode, K. M., Johns, A. R., Christensen-Dalsgaard, J.
643 and Bee, M. A.** (2014). Spatial hearing in Cope's gray treefrog: II. Frequency-dependent
644 directionality in the amplitude and phase of tympanum vibrations. *Journal of Comparative
645 Physiology A* **200**, 285-304.
- 646 **Carr, C. E. and Christensen-Dalsgaard, J.** (2016). Evolutionary trends in directional
647 hearing. *Current Opinion in Neurobiology* **40**, 111-117.
- 648 **Christensen-Dalsgaard, J.** (2005). Directional hearing in nonmammalian tetrapods. In
649 *Sound Source Localization*, vol. 25 eds. A. N. Popper and R. R. Fay), pp. 67-123. New York:
650 Springer.
- 651 **Christensen-Dalsgaard, J.** (2011). Vertebrate pressure-gradient receivers. *Hearing
652 Research* **273**, 37-45.
- 653 **Christensen-Dalsgaard, J. and Manley, G. A.** (2005). Directionality of the lizard ear.
654 *Journal of Experimental Biology* **208**, 1209-1217.
- 655 **Christensen-Dalsgaard, J. and Manley, G. A.** (2008). Acoustical coupling of lizard
656 eardrums. *Journal of the Association for Research in Otolaryngology* **9**, 407-416.

- 657 **Christensen-Dalsgaard, J., Tang, Y. Z. and Carr, C. E.** (2011). Binaural processing by
658 the gecko auditory periphery. *Journal of Neurophysiology* **105**, 1992-2004.
- 659 **Chung, S. H., Pettigrew, A. G. and Anson, M.** (1981). Hearing in the frog: Dynamics of
660 the middle ear. *Proceedings of the Royal Society B-Biological Sciences* **212**, 459-485.
- 661 **De Jongh, H. and Gans, C.** (1969). On the mechanism of respiration in the bullfrog,
662 *Rana catesbeiana*: A reassessment. *Journal of Morphology* **127**, 259-289.
- 663 **Eggermont, J. J.** (1988). Mechanisms of sound localization in anurans. In *The Evolution*
664 *of the Amphibian Auditory System*, eds. B. Fritzsche M. J. Ryan W. Wilczynski T. Hetherington
665 and W. Walkowiak), pp. 307-336. New York: John Wiley & Sons.
- 666 **Ehret, G. and Capranica, R. R.** (1980). Masking patterns and filter characteristics of
667 auditory nerve fibers in the green treefrog (*Hyla cinerea*). *Journal of Comparative Physiology*
668 **141**, 1-12.
- 669 **Ehret, G. and Gerhardt, H. C.** (1980). Auditory masking and effects of noise on
670 responses of the green treefrog (*Hyla cinerea*) to synthetic mating calls. *Journal of Comparative*
671 *Physiology A* **141**, 13-18.
- 672 **Ehret, G., Keilwerth, E. and Kamada, T.** (1994). The lung-eardrum pathway in three
673 treefrog and four dendrobatid frog species: Some properties of sound transmission. *Journal of*
674 *Experimental Biology* **195**, 329-343.
- 675 **Ehret, G., Moffat, A. J. M. and Capranica, R. R.** (1983). Two-tone suppression in
676 auditory nerve fibers of the green treefrog (*Hyla cinerea*). *Journal of the Acoustical Society of*
677 *America* **73**, 2093-2095.
- 678 **Ehret, G., Tautz, J., Schmitz, B. and Narins, P. M.** (1990). Hearing through the lungs:
679 Lung-eardrum transmission of sound in the frog *Eleutherodactylus coqui*. *Naturwissenschaften*
680 **77**, 192-194.
- 681 **Feng, A. S. and Capranica, R. R.** (1978). Sound localization in anurans II. Binaural
682 interaction in superior olivary nucleus of the green tree frog (*Hyla cinerea*). *Journal of*
683 *Neurophysiology* **41**, 43-54.
- 684 **Feng, A. S., Gerhardt, H. C. and Capranica, R. R.** (1976). Sound localization behavior
685 of the green treefrog (*Hyla cinerea*) and the barking treefrog (*Hyla gratiosa*). *Journal of*
686 *Comparative Physiology* **107**, 241-252.
- 687 **Feng, A. S., Hall, J. C. and Siddique, S.** (1991). Coding of temporal parameters of
688 complex sounds by frog auditory nerve fibers. *Journal of Neurophysiology* **65**, 424-445.
- 689 **Gerhardt, H. C.** (1974). The significance of some spectral features in mating call
690 recognition in the green treefrog (*Hyla cinerea*). *Journal of Experimental Biology* **61**, 229-241.

- 691 **Gerhardt, H. C.** (1976). Significance of two frequency bands in long distance vocal
692 communication in the green treefrog. *Nature* **261**, 692-694.
- 693 **Gerhardt, H. C.** (1978a). Discrimination of intermediate sounds in a synthetic call
694 continuum by female green tree frogs. *Science* **199**, 1089-1091.
- 695 **Gerhardt, H. C.** (1978b). Mating call recognition in the green treefrog (*Hyla cinerea*):
696 Significance of some fine-temporal properties. *Journal of Experimental Biology* **74**, 59-73.
- 697 **Gerhardt, H. C.** (1981). Mating call recognition in the green treefrog (*Hyla cinerea*):
698 Importance of two frequency bands as a function of sound pressure level. *Journal of*
699 *Comparative Physiology* **144**, 9-16.
- 700 **Gerhardt, H. C.** (1987). Evolutionary and neurobiological implications of selective
701 phonotaxis in the green treefrog, *Hyla cinerea*. *Animal Behaviour* **35**, 1479-1489.
- 702 **Gerhardt, H. C.** (1991). Female mate choice in treefrogs: static and dynamic acoustic
703 criteria. *Animal Behaviour* **42**, 615-635.
- 704 **Gerhardt, H. C.** (2001). Acoustic communication in two groups of closely related
705 treefrogs. *Advances in the Study of Behavior* **30**, 99-167.
- 706 **Gerhardt, H. C.** (2005). Acoustic spectral preferences in two cryptic species of grey
707 treefrogs: Implications for mate choice and sensory mechanisms. *Animal Behaviour* **70**, 39-48.
- 708 **Gerhardt, H. C. and Bee, M. A.** (2007). Recognition and localization of acoustic signals.
709 In *Hearing and Sound Communication in Amphibians*, vol. 28 eds. P. M. Narins A. S. Feng R. R.
710 Fay and A. N. Popper), pp. 113-146. New York: Springer.
- 711 **Gerhardt, H. C., Daniel, R. E., Perrill, S. A. and Schramm, S.** (1987). Mating behavior
712 and male mating success in the green treefrog. *Animal Behaviour* **35**, 1490-1503.
- 713 **Gerhardt, H. C. and Höbel, G.** (2005). Mid-frequency suppression in the green treefrog
714 (*Hyla cinerea*): mechanisms and implications for the evolution of acoustic communication.
715 *Journal of Comparative Physiology A* **191**, 707-714.
- 716 **Gerhardt, H. C. and Huber, F.** (2002). Acoustic communication in insects and anurans:
717 common problems and diverse solutions. Chicago: Chicago University Press.
- 718 **Gerhardt, H. C., Martinez-Rivera, C. C., Schwartz, J. J., Marshall, V. T. and Murphy,**
719 **C. G.** (2007). Preferences based on spectral differences in acoustic signals in four species of
720 treefrogs (Anura: Hylidae). *Journal of Experimental Biology* **210**, 2990-2998.
- 721 **Gerhardt, H. C. and Rheinlaender, J.** (1982). Localization of an elevated sound source
722 by the green tree frog. *Science* **217**, 663-664.
- 723 **Greenhouse, S. W. and Geisser, S.** (1959). On methods in the analysis of profile data.
724 *Psychometrika* **24**, 95-112.

- 725 **Gridi-Papp, M., Feng, A. S., Shen, J. X., Yu, Z. L., Rosowski, J. J. and Narins, P. M.**
726 (2008). Active control of ultrasonic hearing in frogs. *Proceedings of the National Academy of*
727 *Sciences of the United States of America* **105**, 11014-11019.
- 728 **Ho, C. C. K. and Narins, P. M.** (2006). Directionality of the pressure-difference receiver
729 ears in the northern leopard frog, *Rana pipiens pipiens*. *Journal of Comparative Physiology A*
730 **192**, 417-429.
- 731 **Höbel, G. and Gerhardt, H. C.** (2003). Reproductive character displacement in the
732 acoustic communication system of green tree frogs (*Hyla cinerea*). *Evolution* **57**, 894-904.
- 733 **Jørgensen, M. B.** (1991). Comparative studies of the biophysics of directional hearing in
734 anurans. *Journal of Comparative Physiology A* **169**, 591-598.
- 735 **Jørgensen, M. B. and Gerhardt, H. C.** (1991). Directional hearing in the gray tree frog
736 *Hyla versicolor*: Eardrum vibrations and phonotaxis. *Journal of Comparative Physiology A* **169**,
737 177-183.
- 738 **Jørgensen, M. B., Schmitz, B. and Christensen-Dalsgaard, J.** (1991). Biophysics of
739 directional hearing in the frog *Eleutherodactylus coqui*. *Journal of Comparative Physiology A*
740 **168**, 223-232.
- 741 **Klump, G. M.** (1995). Studying sound localization in frogs with behavioral methods. In
742 *Methods in Comparative Psychoacoustics*, eds. G. M. Klump R. J. Dooling R. R. Fay and W. C. C.
743 Stebbins), pp. 221-233. Basel: Birkhäuser Verlag.
- 744 **Klump, G. M., Benedix, J. H., Gerhardt, H. C. and Narins, P. M.** (2004). AM
745 representation in green treefrog auditory nerve fibers: Neuroethological implications for pattern
746 recognition and sound localization. *Journal of Comparative Physiology A* **190**, 1011-1021.
- 747 **Klump, G. M. and Gerhardt, H. C.** (1989). Sound localization in the barking treefrog.
748 *Naturwissenschaften* **76**, 35-37.
- 749 **Kumar, S., Stecher, G., Suleski, M. and Hedges, S. B.** (2017). TimeTree: A resource
750 for timelines, timetrees, and divergence times. *Molecular Biology and Evolution* **34**, 1812-1819.
- 751 **Lee, N., Christensen-Dalsgaard, J., Schrode, K. M., White, L. A. and Bee, M. A.**
752 (2020). Lung-to-ear sound transmission improves the signal-to-noise ratio for vocal
753 communication in frogs via spectral contrast enhancement. *bioRxiv*.
- 754 **Lee, N., Schrode, K. M. and Bee, M. A.** (2017). Nonlinear processing of a
755 multicomponent communication signal by combination-sensitive neurons in the anuran inferior
756 colliculus. *Journal of Comparative Physiology A* **203**, 749-772.
- 757 **Lopez, P. T. and Narins, P. M.** (1991). Mate choice in the neotropical frog,
758 *Eleutherodactylus coqui*. *Animal Behaviour* **41**, 757-772.

- 759 **Megela-Simmons, A., Moss, C. F. and Daniel, K. M.** (1985). Behavioral audiograms of
760 the bullfrog (*Rana catesbeiana*) and the green tree frog (*Hyla cinerea*). *Journal of the Acoustical*
761 *Society of America* **78**, 1236-1244.
- 762 **Michelsen, A., Jørgensen, M. B., Christensen-Dalsgaard, J. and Capranica, R. R.**
763 (1986). Directional hearing of awake, unrestrained treefrogs. *Naturwissenschaften* **73**, 682-683.
- 764 **Moss, C. F. and Simmons, A. M.** (1986). Frequency selectivity of hearing in the green
765 treefrog, *Hyla cinerea*. *Journal of Comparative Physiology A* **159**, 257-266.
- 766 **Narins, P. and Hillery, C.** (1938). Frequency coding in the inner ear of anuran
767 amphibians. In *Hearing—Physiological Bases and Psychophysics*, pp. 70-76: Springer.
- 768 **Narins, P. M.** (2016). ICE on the road to auditory sensitivity reduction and sound
769 localization in the frog. *Biological Cybernetics* **110**, 263-270.
- 770 **Narins, P. M., Ehret, G. and Tautz, J.** (1988). Accessory pathway for sound transfer in
771 a neotropical frog. *Proceedings of the National Academy of Sciences of the United States of*
772 *America* **85**, 1508-1512.
- 773 **Narins, P. M., Feng, A. S., Fay, R. R. and Popper, A. N.** (2007). *Hearing and Sound*
774 *Communication in Amphibians*. New York: Springer.
- 775 **Narins, P. M. and Smith, S. L.** (1986). Clinal variation in anuran advertisement calls:
776 Basis for acoustic isolation? *Behavioral Ecology and Sociobiology* **19**, 135-141.
- 777 **Narins, P. M. and Wagner, I.** (1989). Noise susceptibility and immunity of phase locking
778 in amphibian auditory nerve fibers. *Journal of the Acoustical Society of America* **85**, 1255-1265.
- 779 **Nogueira, W., Rode, T. and Buchner, A.** (2016). Spectral contrast enhancement
780 improves speech intelligibility in noise for cochlear implants. *Journal of the Acoustical Society of*
781 *America* **139**, 728-739.
- 782 **Oldham, R. S. and Gerhardt, H. C.** (1975). Behavioral isolating mechanisms of
783 treefrogs *Hyla cinerea* and *Hyla gratiosa*. *Copeia* **1975**, 223-231.
- 784 **Penna, M., Capranica, R. R. and Somers, J.** (1992). Hormone-induced vocal behavior
785 and midbrain auditory sensitivity in the green treefrog, *Hyla cinerea*. *Journal of Comparative*
786 *Physiology A* **170**, 73-82.
- 787 **Pinder, A. C. and Palmer, A. R.** (1983). Mechanical properties of the frog ear: Vibration
788 measurements under free- and closed-field acoustic conditions. *Proceedings of the Royal*
789 *Society B-Biological Sciences* **219**, 371-396.
- 790 **Rheinlaender, J., Gerhardt, H. C., Yager, D. D. and Capranica, R. R.** (1979).
791 Accuracy of phonotaxis by the green treefrog (*Hyla cinerea*). *Journal of Comparative Physiology*
792 **133**, 247-255.

- 793 **Rheinlaender, J. and Klump, G. M.** (1988). Behavioral aspects of sound localization. In
794 *The Evolution of the Amphibian Auditory System*, eds. B. Fritsch M. J. Ryan W. Wilczynski
795 and T. Hetherington), pp. 297-305. New York: Wiley & Sons.
- 796 **Rheinlaender, J., Walkowiak, W. and Gerhardt, H. C.** (1981). Directional hearing in
797 the green treefrog: A variable mechanism? *Naturwissenschaften* **68**, 430-431.
- 798 **Römer, H.** (2015). Directional hearing: From biophysical binaural cues to directional
799 hearing outdoors. *Journal of Comparative Physiology A* **201**, 87-97.
- 800 **Römer, H. and Schmidt, A. K. D.** (2016). Directional hearing in insects with internally
801 coupled ears. *Biological Cybernetics* **110**, 247-254.
- 802 **Ronken, D. A.** (1990). Basic properties of auditory-nerve responses from a 'simple' ear:
803 The basilar papilla of the frog. *Hearing Research* **47**, 63-82.
- 804 **Rose, G. J. and Capranica, R. R.** (1985). Sensitivity to amplitude modulated sounds in
805 the anuran auditory nervous system. *Journal of Neurophysiology* **53**, 446-465.
- 806 **Ryan, M. J.** (2001). *Anuran Communication*. Washington D.C.: Smithsonian Institution
807 Press.
- 808 **Schneider, J. G.** (1799). *Historia Amphibiorum Naturalis et Literariae. Fasciculus*
809 *Primus. Continens Ranas, Calamitas, Bufones, Salamandras et Hydros in Genera et Species*
810 *Descriptos Notisque suis Distinctos*. Jena: Friederici Frommanni.
- 811 **Schwartz, J. J. and Bee, M. A.** (2013). Anuran acoustic signal production in noisy
812 environments. In *Animal Communication and Noise*, (ed. H. Brumm), pp. 91-132. New York:
813 Springer.
- 814 **Shen, J. X., Feng, A. S., Xu, Z. M., Yu, Z. L., Arch, V. S., Yu, X. J. and Narins, P. M.**
815 (2008). Ultrasonic frogs show hyperacute phonotaxis to female courtship calls. *Nature* **453**, 914-
816 916.
- 817 **Simmons, A. M.** (1988). Selectivity for harmonic structure in complex sounds by the
818 green treefrog (*Hyla cinerea*). *Journal of Comparative Physiology A* **162**, 397-403.
- 819 **Simmons, A. M.** (2013). "To Ear is Human, to Frogive is Divine": Bob Capranica's
820 legacy to auditory neuroethology. *Journal of Comparative Physiology A* **199**, 169-182.
- 821 **Simmons, A. M., Buxbaum, R. C. and Mirin, M. P.** (1993). Perception of complex
822 sounds by the green treefrog, *Hyla cinerea*: Envelope and fine-structure cues. *Journal of*
823 *Comparative Physiology A* **173**, 321-327.
- 824 **Simpson, A. M., Moore, B. C. J. and Glasberg, B. R.** (1990). Spectral enhancement to
825 improve the intelligibility of speech in noise for hearing-impaired listeners. *Acta Oto-*
826 *Laryngologica*, 101-107.

- 827 **Ursprung, E., Ringler, M. and Hödl, W.** (2009). Phonotactic approach pattern in the
828 neotropical frog *Allobates femoralis*: A spatial and temporal analysis. *Behaviour* **146**, 153-170.
- 829 **van Hemmen, J. L., Christensen-Dalsgaard, J., Carr, C. E. and Narins, P. M.** (2016).
830 Animals and ICE: Meaning, origin, and diversity. *Biological Cybernetics* **110**, 237-246.
- 831 **Vélez, A., Schwartz, J. J. and Bee, M. A.** (2013). Anuran acoustic signal perception in
832 noisy environments. In *Animal Communication and Noise*, (ed. H. Brumm), pp. 133-185. New
833 York: Springer.
- 834 **Vlaming, M. S. M. G., Aertsen, A. M. H. J. and Epping, W. J. M.** (1984). Directional
835 hearing in the grass frog (*Rana temporaria* L.): I. Mechanical vibrations of tympanic membrane.
836 *Hearing Research* **14**, 191-201.
- 837 **Ward, J. L., Love, E. K., Vélez, A., Buerkle, N. P., O'Bryan, L. R. and Bee, M. A.**
838 (2013). Multitasking males and multiplicative females: Dynamic signalling and receiver
839 preferences in Cope's grey treefrog. *Animal Behaviour* **86**, 231-243.
- 840 **Wells, K. D. and Schwartz, J. J.** (2007). The behavioral ecology of anuran
841 communication. In *Hearing and Sound Communication in Amphibians*, vol. 28 eds. P. M. Narins
842 A. S. Feng R. R. Fay and A. N. Popper), pp. 44-86. New York: Springer.
- 843 **Wilczynski, W., Resler, C. and Capranica, R. R.** (1987). Tympanic and extratympanic
844 sound transmission in the leopard frog. *Journal of Comparative Physiology A* **161**, 659-669.
845

Table 1. Summary of maximum vibration amplitude differences (VADs) in three states of lung inflation			
Maximum VAD	Inflated	Deflated	Reinflated
Amplitude (dB)	15.5 ± 0.6	11.5 ± 0.4	14.5 ± 0.6
Frequency (Hz)	1486 ± 42	1255 ± 72	1402 ± 77
Ipsilateral angle (°)	99 ± 16	108 ± 3	115 ± 7
Contralateral angle (°)	-49 ± 4	-88 ± 5	-67 ± 4

The mean and 95% confidence intervals are shown for the amplitude of the maximum VADs across the three states of lung inflation, the frequencies at which they occurred, and the ipsilateral and contralateral angles across which they were computed.

Table 2. Summary of the maximum interaural vibration amplitude differences (IVADs) in three states of lung inflation												
	Magnitude of maximum IVAD (dB)				Frequency of maximum IVAD (Hz)				Angle of maximum IVAD (°)			
Lung condition	Median	Mean	SD	CI	Median	Mean	SD	CI	Median	Mean	SD	CI
Inflated	12.1	12.4	2.7	1.1	1550	1607.5	792.9	339.0	90	82.9	18.7	8.0
Deflated	10.6	11.2	2.4	1.0	1250	1689.9	1639.1	701.0	90	100.0	19.7	8.4
Reinflated	12.1	12.5	2.4	1.0	1450	1579.0	1439.7	615.8	90	95.7	22.5	9.6

The median, mean, standard deviation (SD), and 95% confidence intervals (CI) are shown for the magnitude of the maximum IVAD, and the frequency and sound incidence angle at which the maximum occurred, based on a sample of 21 subjects.

Table 3. Relationships between frequencies of the “dip” in tympanum transfer functions, the spectral peaks of conspecific calls, the peak resonance of the lungs, and vibration amplitude differences (VADs)							
Species	Lower spectral peak (Hz)	Dip Frequency (Hz)	Lung resonance frequency (Hz)	Higher spectral peak (Hz)	VAD at dip frequency (dB)	VAD at call frequencies (dB)	References
<i>Hyla cinerea</i>	834	1400 to 2200	1400 to 1850	2730	12 to 16	6 to 10	This study; Lee et al. (2020)
<i>Hyla gratiosa</i>	410 to 500	700 to 1300	700 to 900	1680-2150	15 to 25	< 10	Jørgensen (1991); Oldham and Gerhardt (1975)
<i>Hyla versicolor</i>	1100	1300 to 1800	1300 to 1600	2200	15 to 25	< 6	Jørgensen and Gerhardt (1991)
<i>Hyla chrysoscelis</i>	1250	1600 to 1900	1400	2500	10 to 15	< 10	Caldwell et al. (2014); (Ward et al., 2013)
<i>Eleutherodactylus coqui</i>	1500	1720	1500 to 1800	2400-2700	10 to 15	5 to 6	Jørgensen et al. (1991); (Narins and Smith, 1986); (Lopez and Narins, 1991)
<i>Rana temporaria</i>	350 to 500	600 to 1000	650 to 700	1200	10 to 15	< 5	Jørgensen (1991); (Brzoska et al., 1977)

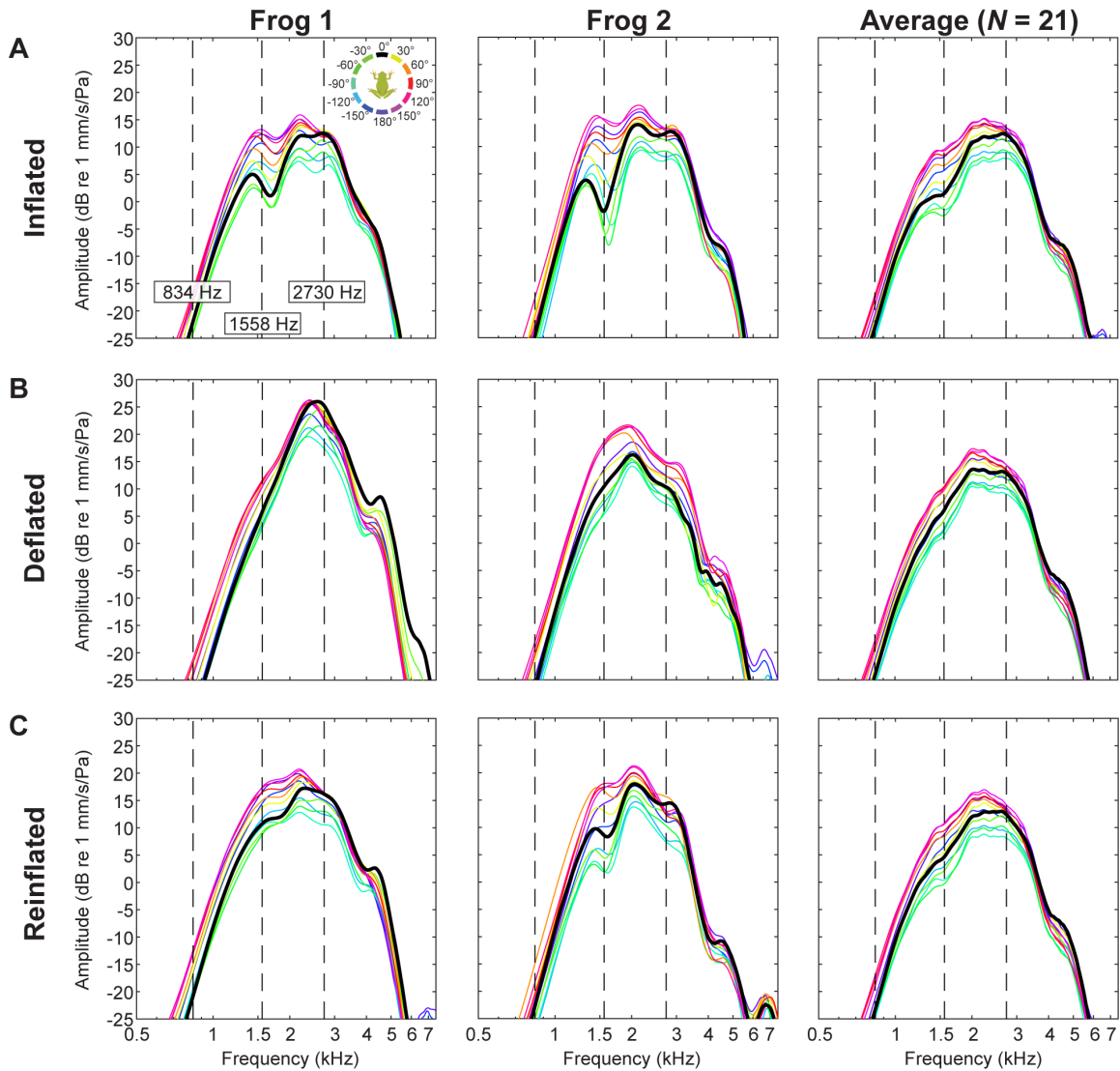


Fig. 1. Response of the tympanum to free-field sound in three states of lung inflation.

Shown here are tympanum transfer functions measured in response to a frequency modulated (FM) sweep broadcast from 12 sound incidence angles in azimuth (0° , $\pm 30^\circ$, $\pm 60^\circ$, $\pm 90^\circ$, $\pm 120^\circ$, $\pm 150^\circ$, 180°). Transfer functions at each angle were generated by dividing the vibration amplitude spectrum measured with the laser by the corresponding sound spectrum measured with the probe microphone adjacent to the measured tympanum. Data are presented for two representative frogs and averaged over 21 frogs and are shown separately for the (A) inflated, (B), deflated, and (C) reinflated states of lung inflation. Vertical dashed lines depict frequencies of the two spectral peaks in conspecific advertisement calls (834 Hz and 2730 Hz) and the peak resonance frequency of the lungs (1559 Hz) (Lee et al., 2020).

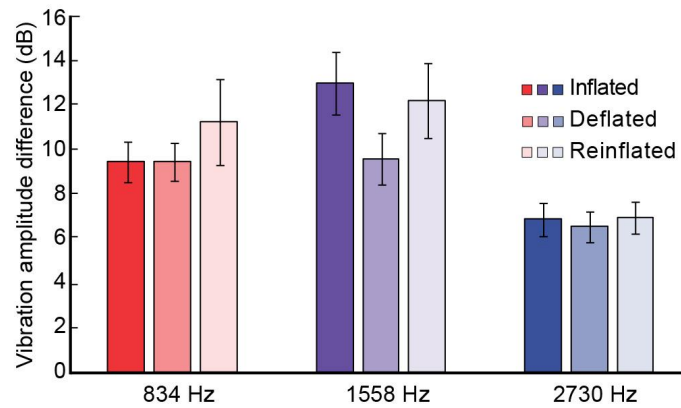


Fig. 2. Impacts of lung inflation on the vibration amplitude difference (VAD). Shown here are the mean (\pm 95% CIs) VADs measured in three states of lung inflation (inflated, deflated, and reinflated) at frequencies corresponding to the two spectral components emphasized in conspecific calls (834 Hz and 2730 Hz) and at the peak resonance frequency of the lungs (1558 Hz).

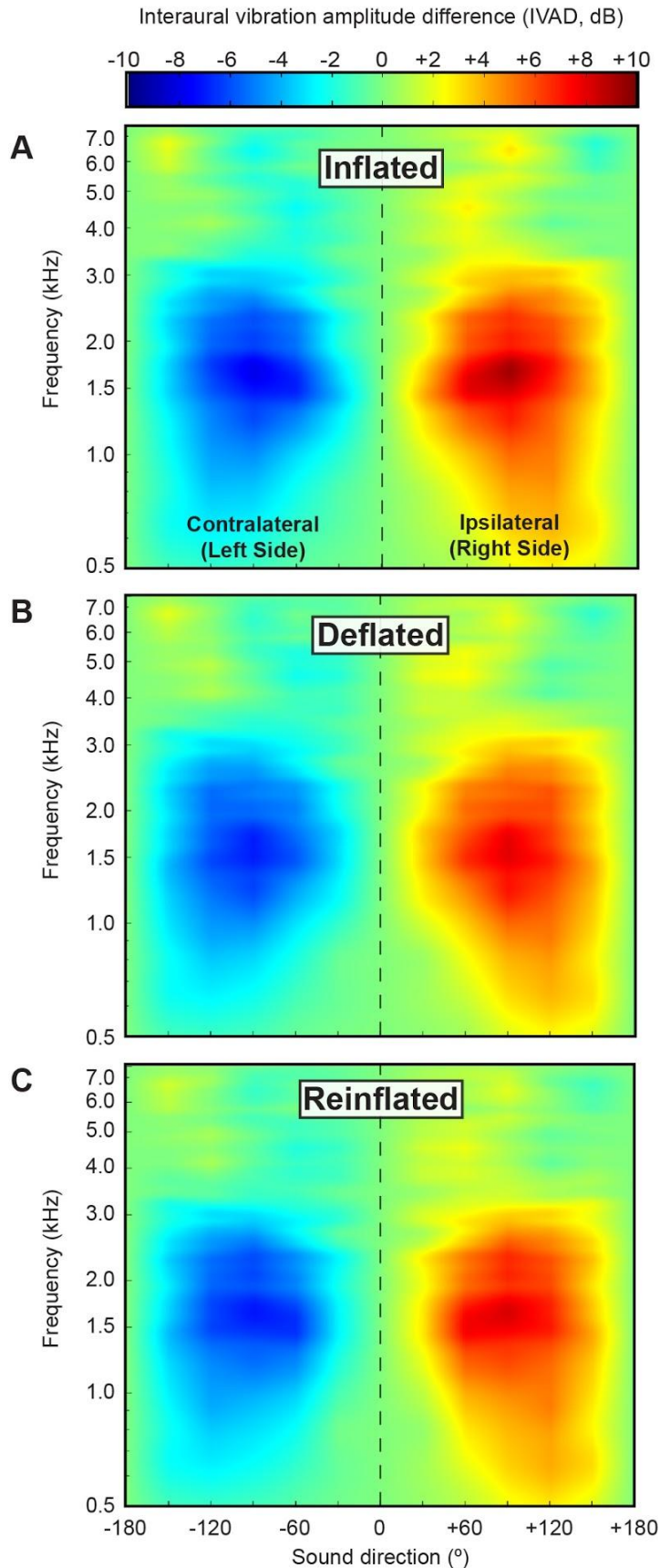


Fig. 3. Interaural vibration amplitude differences (IVADs).

Shown here are the mean interaural vibration amplitude differences (IVADs; $N = 21$) in response to a frequency-modulated (FM) sweep as a function of frequency and sound incidence angle. In each plot, values are interpolated across frequency and sound incidence angle and averaged over 21 subjects. Data are shown separately for the (A) inflated, (B) deflated, and (C) reinflated states of lung inflation. IVADs are measures of binaural disparity that assume bilateral symmetry. These heatmap plots of IVADs depict the differential stimulation of the ipsilateral (right) side, with positive values (red color) corresponding to sounds arising in the ipsilateral hemifield and negative values (blue color) corresponding to sounds arising in the contralateral hemifield.

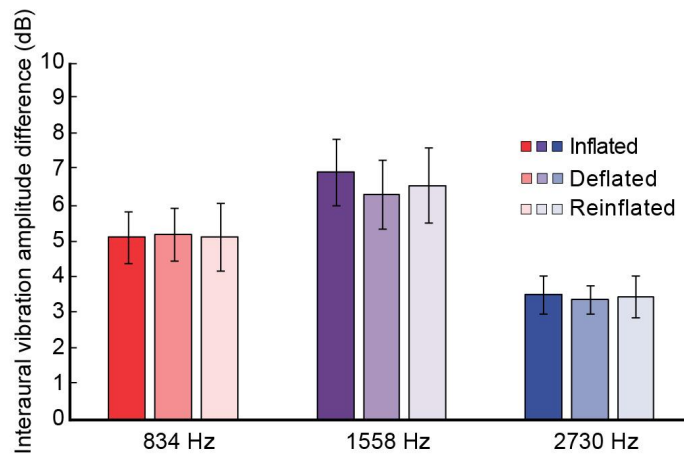


Fig. 4. Impacts of lung inflation on the interaural vibration amplitude difference (IVAD).

Shown here are the mean (\pm 95% CIs) IVADs measured in three states of lung inflation (inflated, deflated, and reinflated) at frequencies corresponding to the two spectral components emphasized in conspecific calls (834 Hz and 2730 Hz) and at the peak resonance frequency of the lungs (1558 Hz). Values are averaged over the measured sound incidence angles of 30°, 60°, 90°, 120°, and 150°.

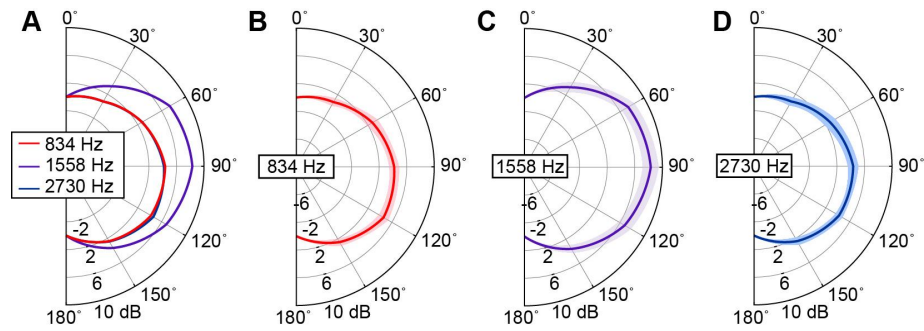


Fig. 5. Interaural vibration amplitude differences (IVADs) as functions of frequency and sound incidence angle. (A) Half-polar plot comparing the magnitude of the mean IVAD in the inflated condition as a function of sound incidence angle for two frequencies emphasized in conspecific advertisement calls (834 Hz and 2730 Hz) and at the mean peak frequency of the lung resonance (1558 Hz). IVADs were greatest at all three frequencies when sounds were presented from lateral positions. (B-C) Half polar plots showing the mean (line) \pm 95% confidence interval (shaded region) IVAD separately for each frequency as a function of sound incidence angle.

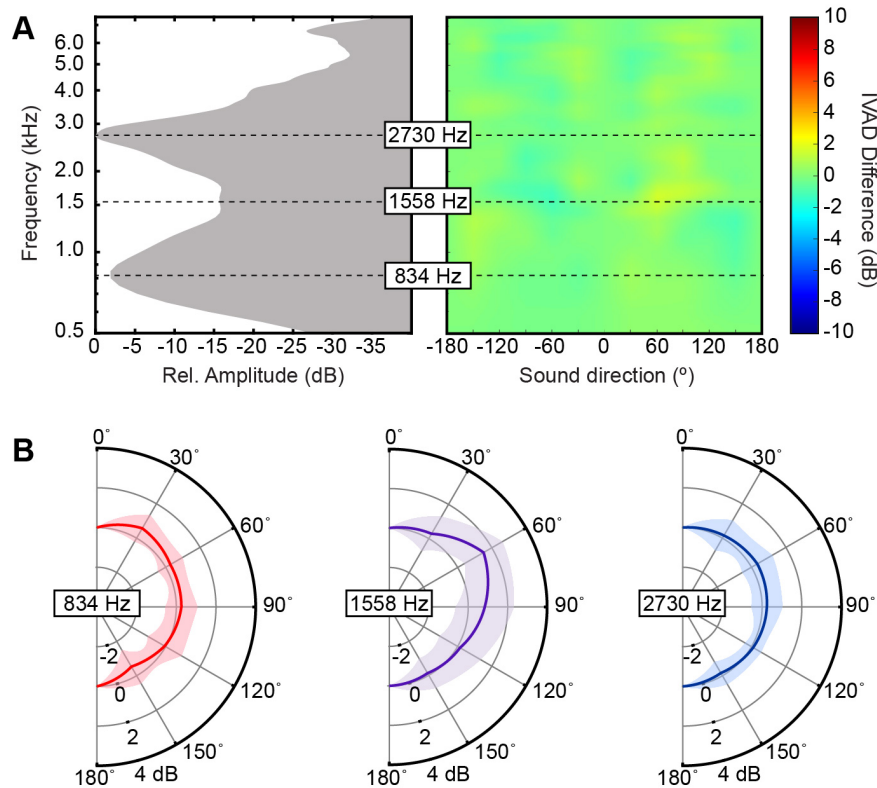


Fig. 6. Relationship between the advertisement call spectrum and lung mediated differences in interaural vibration amplitude differences (IVADs). (A) On the left is shown the frequency spectrum of conspecific advertisement calls depicting relative amplitude as a function of frequency (redrawn from Lee et al., 2020). On the right is shown a heatmap of the differences in IVADs between the inflated and deflated conditions (inflated - deflated). Note that the call spectrum is rotated 90° counterclockwise relative to customary depictions of call spectra in order to facilitate comparisons with lung mediated differences in IVADs. The mean spectral peaks in the call (834 Hz and 2730 Hz) and the mean peak frequency of the lung resonance are highlighted. (B) Half polar plots depicting the magnitude (mean ± 95% CI) of the difference in IVADs between the inflated and deflated conditions as a function of sound incidence angle for the three frequencies highlighted in (A).